Langmuir

Article

pubs.acs.org/Langmuir

Chunks of Charge: Effects at Play in the Assembly of Macromolecules at Fluid Surfaces

Ellen J. Robertson and Geraldine L. Richmond*

Department of Chemistry, University of Oregon, Eugene, Oregon 97403, United States

ABSTRACT: Large macromolecules with hydrophobic backbones are known to assemble at the interface between immiscible liquids. This assembly is often unpredictable because of the subtle interplay among hydrophobic interactions, hydrophilic solvation, structural constraints, and the thermodynamics of adsorption. In these studies, we employ vibrational sum frequency spectroscopy and interfacial tension measurements to study the assembly of a simple polyelectrolyte, poly(methacrylic acid), as it assembles at the interface between two immiscible liquids, specifically, carbon tetrachloride and water. By adjusting the polyelectrolyte charge through pH studies and the polymer size through molecular weight studies, we demonstrate that charge accumulation in segments of the polymer chains is a critical factor in macromolecular interfacial adsorption and desorption. The results have implications for related charged macromolecules whose ability to assemble between two immiscible fluid media is essential for many biological processes, water remediation efforts, and enhanced oil recovery.

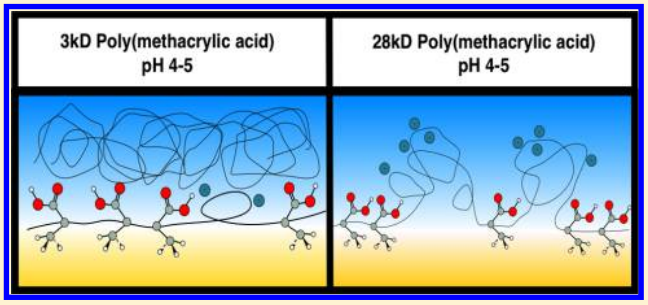

INTRODUCTION

Carboxylic acids are important functional groups that comprise ionizable interfacial macromolecules. For instance, carboxylic acids are present in proteins in the form of glutamic and aspartic acid, and interactions with proteins and fluid cell surfaces are often essential for biological processes.[1] Carboxylic acids also comprise much of natural organic matter in the form of humic and fulvic acids, and these materials are often utilized in oil recovery and water remediation technologies.[2−6] The fact that the carboxylic acid functional group is pH-tunable allows it to be engineered into "smart" materials that are able to assemble at interfaces for a variety of technologies.[7,8] Fatty acids are a classic example of carboxylic acid-containing macromolecules that are able to target fluid interfaces for applications ranging from emulsion stabilization to water remediation to monolayer formation.

Fluid interfaces are a platform for a variety of important processes that include interface-catalyzed reactions,[9,10] ion transfer,[11,12] nanoparticle synthesis and assembly,[13−15] oil recovery and water remediation,[16] and biological processes that occur at the interface between a fluid cell membrane and water.[17,18] These processes often depend on the adsorption and assembly of ionizable macromolecules to the interface between a nonpolar fluid and water.

Previously, work has been done to understand the adsorption and assembly of alkyl surfactants at oil−water interfaces.[19,20] It is well known that a key feature that drives the adsorption of these surfactants to the interface is their amphiphilic nature, with highly hydrophilic headgroups preferring the aqueous phase and highly hydrophobic tails preferring the oil phase. Previous pH studies from our laboratory have shown that the charge of alkyl surfactants plays a large role in their adsorption and assembly to an oil−water interface, and specifically, the charge of the carboxylate headgroup is essential for the formation of an ordered monolayer at the oil−water interface.[21]

As alkyl surfactant interfacial behavior has become increasingly well understood, interest has shifted to discovering how the behavior of macromolecular charging dictates the adsorption and assembly of carboxylic acid-containing polymers at similar oil−water interfaces. Unlike alkyl surfactants that are composed of an ionizable, hydrophilic headgroup on one end and an oily hydrocarbon tail on the opposite end, carboxylic acid-containing polymers are weak polyelectrolytes in which several ionizable groups are linked together along a hydrophobic backbone. In this case, there is an even distribution of hydrophobic groups (methyl and methylene) and hydrophilic groups (either carboxylic acid or carboxylate) along the length of the molecule. The balance between polymer chain hydrophobicity and hydrophilicity and how charging plays a role in interfacial behavior has the potential to be quite different for carboxylic acid-containing polymers than for alkyl surfactants. Although several experimental and theoretical studies have detailed the behavior of carboxylic acid-containing polymers in the bulk,[22−24] at planar solid[25−27] and particle[28−30] surfaces, and at fluid interfaces in the presence of oppositely charged surfactants,[31−33] few have focused on the molecular-level details concerning the adsorption and assembly of these polyelectrolytes to the interface between polar and nonpolar fluids.[34−37]

Received: June 3, 2013
Revised: July 25, 2013
Published: August 2, 2013

In this work, both vibrational sum frequency (VSF) spectroscopy and interfacial tension measurements are used to study how the charging behavior of a carboxylic acid-containing polymer, the syndiotactic isomer of poly(methacrylic acid) (sPMA) (Figure 1), affects its adsorption

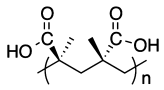

Figure 1. Structure of sPMA (n = 17 or 163).

to and assembly at the carbon tetrachloride–water (CCl_4–H_2O) interface. Such simple polyelectrolytes have been shown to be good models for naturally occurring polycarboxylic acids such as peptides[38] and humic substances,[39] whose applications at fluid interfaces are quite relevant. For instance, humic substances have been shown to be promising materials in the remediation of groundwater contaminated by chlorinated solvents.[6] Our studies thus model an important environmental system, with CCl_4 serving as an appropriate model for environmental toxins. Through variation of the pH in the aqueous phase, the number of charges per polymer chain is varied; at low pH, most of the carboxylic acid groups are neutral, and as the pH is increased, the number of charges per chain increases. Also explored, herein, is the effect of the number of ionizable groups per chain on polymer interfacial behavior, using sPMA polymers with molecular weights of 3 kD and 28 kD. By keeping the carboxylate group (monomer) concentrations constant for the different molecular weight samples, larger polymer samples contain fewer chains than the smaller polymer. At similar pH values, the larger polymer chains will accumulate a greater number of charges than the smaller polymer chains and, as a consequence of their flexibility, can have enhanced charge cooperativity compared to that of shorter chains. How these "chunks of charge" impact the assembly of these macromolecules is demonstrated for the first time in these studies.

EXPERIMENTAL SECTION

Sum Frequency Experiment and Background. VSF spectroscopy is a powerful technique that gives molecular-level information specific to interfaces. Under the dipole approximation, sum frequency generation is forbidden in any media possessing inversion symmetry, as is generally true for bulk media. A break in symmetry occurs at the interface of centrosymmetric bulk media, making VSF spectroscopy an inherently surface-specific technique.

The laser system used for these studies has been described in detail elsewhere.[40] The laser and OPO/OPA/DFG systems were commercial systems purchased from Ekspla. Briefly, 1064 nm laser pulses of ~30 ps duration and 10 Hz repetition rate were generated from a flashlamp-pumped Nd:YAG crystal, with mode-locking accomplished with a solid-state saturable absorber. After amplification, the 1064 nm beam was split, and part was passed through a second harmonic crystal to generate 532 nm pulses. The rest was sent to the OPO/OPA/DFG system. The 532 nm beam was also split, with a small portion sent to the interface and the rest sent to the OPG/OPA/DFG system, where it was used with the 1064 nm beam to generate a tunable infrared beam that was sent to the interface.

Using total internal reflection (TIR) geometry, both the visible and tunable infrared beams were passed through the carbon tetrachloride layer to the interface at their respective TIR angles. The beams were overlapped in space and time, and the resulting sum frequency signal was passed through a monochromator (model MS2001) and detected with a PMT (Hamamatsu R7899). All spectra are at least an average of 300 shots per point.

The detected sum frequency signal intensity, $I(\omega_{SFG})$, is proportional to the square of the effective second-order susceptibility, $\chi^{(2)}_{eff}$, and the intensities of the incident visible and IR beams, $I(\omega_{vis})$ and $I(\omega_{IR})$, according to eq 1.

$$I(\omega_{SFG}) \propto |\chi^{(2)}_{eff}|^2 I(\omega_{vis})\, I(\omega_{IR}) \tag{1}$$

Here, $\chi^{(2)}_{eff}$ is related to the actual $\chi^{(2)}$ through the Fresnel coefficients and the unit polarization vectors. $\chi^{(2)}$ is composed of a nonresonant component, $\chi^{(2)}_{NR}$, that depends on the polarizability of the interfacial molecules and a sum of resonant components, $\chi^{(2)}_{R_v}$, that arise when the infrared beam frequency is coincident with a sum frequency active vibrational transition of an interfacial molecule, as represented in eq 2.

$$\chi^{(2)} = \chi^{(2)}_{NR} + \sum_v \chi^{(2)}_{R_v} \tag{2}$$

For the liquid–liquid interface studied here, $\chi^{(2)}_{NR}$ is essentially zero. The resonant components of $\chi^{(2)}$ depend upon both the number density of interfacial molecules, N, and the orientationally averaged molecular hyperpolarizability, $\langle\beta_v\rangle$, according to eq 3.

$$\chi^{(2)}_{R_v} = \frac{N}{\varepsilon_0}\langle\beta_v\rangle \tag{3}$$

To generate the sum frequency signal, molecules present at the interface must have a net orientation. Different polarization combinations of the incident and detected beams can be employed to probe different components of the $\chi^{(2)}_{R_v}$ tensor. For these studies, the ssp polarization scheme (s, sum frequency; s, visible; and p, infrared beam polarizations, respectively) was used to probe vibrational modes having components of their IR transition moment normal to the plane of the interface.

All spectra presented were normalized by dividing the raw spectra by nonresonant gold spectra in the corresponding spectral regions to account for changes in the spatial and temporal overlap of the incident beams as the IR frequency is tuned. The resulting spectra were fit using a convolution of a Gaussian and Lorentzian distribution described by Bain et al.,[41] shown in eq 4.

$$\left|\chi^{(2)}(\omega_{SFG})\right|^2 = \left|\sum_v \int_{-\infty}^{\infty} \frac{A_v e^{i\varphi_v} e^{-[(\omega_L-\omega_v)/\Gamma_v]^2}}{\omega_L - \omega_{IR} + i\Gamma_L}\, d\omega_L\right|^2 \tag{4}$$

This line shape takes into account both homogeneous broadening due to the inherent nature of the transition and inhomogeneous broadening due to the local environments of the molecules. For the fits, the Lorentzian line widths were held at constant values consistent with typical vibrational lifetimes,[42−45] and the Gaussian line widths were allowed to vary to account for the wide array of complex molecular environments.

Interfacial Tension Measurements. Interfacial tension measurements were conducted using the pendant drop method in which the shape of a liquid drop suspended in a bulk medium is determined by the interfacial tension. The instrument, purchased from KSV, consisted of a camera and a monochromatic LED back light to ensure good photoresolution. Interfacial tension measurements were performed by suspending an aqueous drop in a 1 × 1 cm^2 quartz cuvette containing carbon tetrachloride. The aqueous drop was formed from a 1 mL gastight Hamilton syringe with an affixed Kel-F hub hooked needle. The syringe plunger was held in place with a Hamilton repeating dispenser. Daily, the interfacial tension of the neat CCl_4–H_2O interface was measured to ensure the cleanliness of the syringe and cuvette. Samples were measured by taking a photograph of the drop once a minute until the interfacial tension did not change with time. Using the software that was provided with the instrument, we first fit the shape of the drop to the Laplace–Young equation to determine the shape factor β. The surface tension γ was subsequently calculated using the following equation.

dx.doi.org/10.1021/la4021096 | Langmuir 2013, 29, 10980−10989

$$\gamma = \frac{\Delta\rho g R_0^{(2)}}{\beta} \quad (5)$$

Here, $\Delta\rho$ is the difference in the density of water compared to that of carbon tetrachloride, g is the gravitational constant, and R_0^2 is the square of the radius of the drop curvature at the drop apex.

Materials and Sample Preparation. Syndiotactic poly(methacrylic acid) samples (3 kD, PDI = 1.16; 28 kD, PDI = 1.2) were purchased from Polymer Source and were used as received. All solutions were prepared using glassware that was soaked in a NoChromix–H_2SO_4 bath for at least 12 h and subsequently rinsed copiously with water from an E-pure filtration system that had a resistivity of 18.2 MΩ. Polymer stock solutions (100 ppm) were prepared by dissolving either 3 or 28 kD sPMA in water from the E-pure filtration system and then sonicating these solutions in a bath sonicator for ∼10 min. The 5 ppm solutions were prepared from these stock solutions. The pH of these solutions was adjusted using either 1 N NaOH (volumetric standard, purchased from Aldrich) or diluted HCl solutions (prepared from a 37% HCl ACS-grade solution purchased from Sigma-Aldrich). D_2O was purchased from Cambridge Isotopes, and DCl was purchased from Aldrich. The pH values of the solutions were tested with pH paper, with regular verification from an Oakton 110 pH meter. The pH values of the solutions did not significantly change over the time frame of the experiments.

The sample cell was machined from a solid piece of Kel-F, with a CaF_2 window facing the incoming beams and a BK7 window facing the out-going beams. The sample cell, o-rings, and BK7 window were cleaned by soaking in a NoChromix–H_2SO_4 bath for at least 12 h followed by rinsing with the E-Pure water for at least 20 min. The CaF_2 window was soaked in the NoChromix–H_2SO_4 bath for ∼10 min, followed by rinsing with the E-pure water for at least 20 min. A spectrum of a neat CCl_4–H_2O interface was obtained each day after depositing multiple CCl_4–H_2O layers into the cell to ensure cell cleanliness.

RESULTS AND DISCUSSION

Low-Molecular-Weight sPMA. To study the effects of polymer charging on the adsorption behavior of sPMA with a molecular weight of 3 kD, VSF spectra were collected over a range of pH values at the CCl_4–H_2O interface. VSF spectra in the carbonyl stretching region from 1600 to 1900 cm^{-1} are shown in Figure 2A. Given the selection rules for VSF, the presence of the sPMA signal is indicative that it is at the interface. At pH ≥ 5.5, no carbonyl signal was observed, indicative of either no polymer present or completely disordered polymer at the interface.

The spectra in Figure 2A are fit to two peaks in order to reproduce the experimental line shape. The observation of peaks at slightly different vibrational frequencies is due to the carbonyl groups being in different environments. The lower-energy peak near 1730 cm^{-1} is attributed to carbonyl groups in a more water-rich, hydrogen-bonded environment and is consistent with the literature frequencies.[46] The higher-energy peak centered at 1790 cm^{-1} is attributed to carbonyl groups in a more oil-rich environment and is consistent with frequencies observed in FT-IR studies of simple carboxylic acids in bulk CCl_4.[47] Figure 2B shows a representation of the two different carbonyl environments. This picture is consistent with the fits, which show that the two carbonyl peaks are out of phase with each other, indicative of differing orientations of the groups. Previous studies of poly(acrylic acid) (PAA) at the oil–water interface in our laboratory showed the absence of a high-energy peak.[34−36] It is concluded that the appearance of this higher-energy peak for PMA is due to the more hydrophobic nature of this polymer compared to that of PAA, which results in a fraction of the carbonyl groups on PMA existing in a more oil-rich environment compared to that for PAA. Previous VSF spectroscopic studies of the isotactic and atactic isomers of PMA showed a single peak with some asymmetry on the higher-energy side.[35] The results here suggest that the asymmetry could be due to the same effect of having carbonyl groups existing in both water-rich and oil-rich environments.

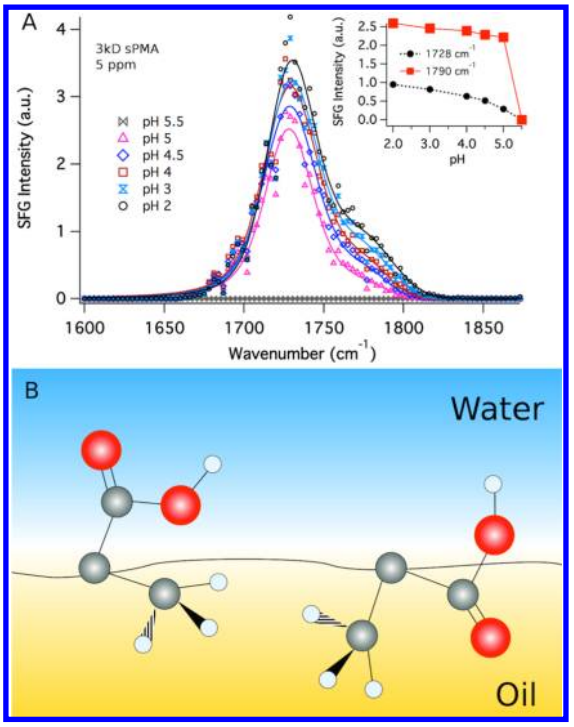

Figure 2. (A) VSF spectra (ssp polarization) of 3 kD sPMA (5 ppm) at different pH values in the carbonyl stretching region. The solid lines are fits to peaks near 1730 and 1790 cm^{-1}. The inset is a plot of the fit amplitudes for both peaks as a function of pH. (B) Cartoon depicting the two different solvation environments of the carbonyl groups corresponding to the peaks near 1730 (left) and 1790 cm^{-1} (right).

The inset in Figure 2A shows the fit amplitudes for both peaks as a function of pH. Signal does not appear until pH <5.5, and gradually the amplitude increases as the pH is further decreased. This suggests that as the pH decreases and more carboxylate groups become protonated the population of oriented carbonyl groups increases at the interface, with functional groups pointing into both the oil and water phases.

Similar to the data in the carbonyl stretching region, the VSF signal due to the polymer is observed only at pH <5.5 in the CH and OH stretching region. At pH 5.5, no peaks appear to indicate that polymer is present at the interface, or if it is, it has no net orientation. Two peaks appear near 3668 and 3200 cm^{-1} and are characteristic of interfacial water at the CCl_4–H_2O interface.[40] As shown in Figure 3A, at pH 5 and below, there are peaks in the region between 2800 and 3000 cm^{-1} resulting from the polymer methylene and methyl stretching modes. The adsorption of 3 kD sPMA to the oil–water interface at a relatively low pH is consistent with previous studies of PAA from this laboratory.[34−36] Adsorption of this polymer to the CCl_4–H_2O interface occurs only at pH ≤5 because polymer charging above this pH makes solvation in water more energetically favorable than interfacial adsorption.

Gradual spectral changes as the pH decreases from 5 to 2 are also observed in the CH and OH stretching region. The spectra of 3 kD sPMA taken in H_2O, which are shown in Figure 3A, are

dx.doi.org/10.1021/la4021096 | Langmuir 2013, 29, 10980−10989

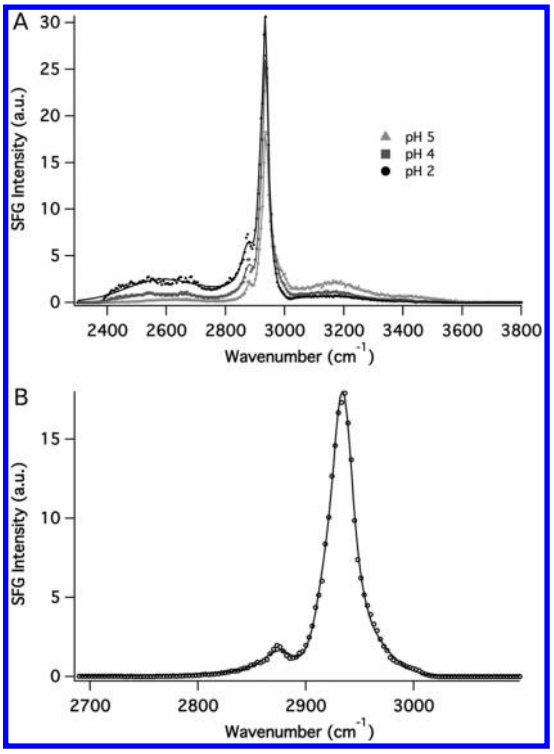

Figure 3. (A) VSF spectra (ssp polarization) of 3 kD sPMA (5 ppm) at different pH values in the CH and OH stretching region. (B) VSF spectra of 3 kD sPMA (5 ppm) in D_2O at pD 2 in the CH stretching region. The solid lines are fits to the data.

very complex. Along with the sharp CH stretching modes between 2800 and 3000 cm^{-1}, due to both the methyl and methylene groups on the polymer, broad peaks are also present on both sides of the CH peaks as a result of the OH stretching modes of both water and the carboxylic acid groups on the polymer. To assist in the fitting and to elucidate the trend in the data, spectra of 3 kD sPMA in D_2O were taken at pD ~2 as shown in Figure 3B. The pD was adjusted using DCl to ensure that most of the carboxylic acid hydrogen atoms would be replaced by deuterium atoms. As can be seen, the broad peaks present in the H_2O spectrum are not present in the D_2O spectrum, indicating that the gradual pH-dependent changes in the 3 kD sPMA spectra taken in water are in part a result of changes in the peaks due to the carboxylic acid and water OH stretching modes.

The water data were fit using a global routine in which all variables were held constant except for peak amplitudes and Gaussian widths. The peak frequencies assigned to the CH stretching modes used in the global routine were constrained to be within the error of those used to fit the D_2O data. Three additional broad peaks were added to account for the OH stretching modes. The peaks due to the CH stretching modes appear near 2880, 2925, 2935, and 2980 cm^{-1} and are assigned to the CH_3 symmetric stretch, the CH_2 asymmetric stretch, the CH_3 Fermi resonance of the methyl symmetric stretch and overtones of the methyl bending modes, and the CH_3 asymmetric stretch, respectively. These frequencies are consistent with sum frequency, IR, and Raman spectroscopic studies of alkanes.[26,43,46,48,49] The peak assigned to the carboxylic acid OH stretching mode appears near 2540 cm^{-1} and is consistent with literature values of simple aqueous carboxylic acid IR studies,[50] whereas the peaks assigned to the water OH stretching modes appearing near 3200 and 3450 cm^{-1} are consistent with literature values from previous VSF spectroscopic studies of more- and less-coordinated water near charged CCl_4–H_2O surfaces, respectively.[51] The water OH signal stems from the charged interfacial carboxylate groups that create a field due to the double-layer effect, which in turn acts to align water molecules at the interface over a longer interfacial distance.[52]

From the results of the spectral fits, it is clear that the decrease in pH from 5 to 2 causes an increase in the amplitude of the peak assigned to the carboxylic acid OH stretching mode (2540 cm^{-1}) and a decrease in the amplitude of the peaks assigned to the water OH stretching modes (3200 and 3400 cm^{-1}). The amplitude increase of the 2540 cm^{-1} peak with pH decrease suggests an increase in the population of oriented carboxylic acid groups at the oil–water interface, consistent with the carbonyl-stretching-mode data. The decrease in amplitudes of the 3200 and 3400 cm^{-1} peaks confirms this picture. The adsorption of the charged 3 kD sPMA to the CCl_4–H_2O interface creates a field that acts to orient water molecules adjacent to the interfacial polymer layer. The neutralization of interfacial charges through the protonation of carboxylate groups results in a decrease in the interfacial field strength and subsequently fewer oriented interfacial water molecules.[21] Additional small changes in peak amplitudes assigned to the CH stretching modes most likely indicate a change in backbone orientation as a result of the increased degree of oriented interfacial carboxylic groups as the pH decreases from 5 to 2.

Despite the evidence for a change in the charging of interfacial polymer as a function of pH seen in the carbonyl, CH, and OH stretching regions, signal was not observed near 1400 cm^{-1} as a result of the carboxylate stretching mode for the pH values studied. This is consistent with previous studies of PAA in this laboratory.[34−36] This is attributed to the carboxylate groups adopting opposite and/or random orientations on chain sections protruding into the water phase to minimize charge–charge repulsions, thus canceling the VSF signal.

The gradual pH-induced changes observed in the VSF spectroscopic data resulting from the change in interfacial polymer charge are somewhat reflected in the interfacial tension data, as shown in Figure 4.

The interfacial tension value of the 3 kD sPMA at pH 5.5 is ~45 mN/m, the same as that for the neat CCl_4–H_2O interface.[53,54] This confirms that at pH 5.5 the 3 kD sPMA does not adsorb to the interface and that the absence of the VSF

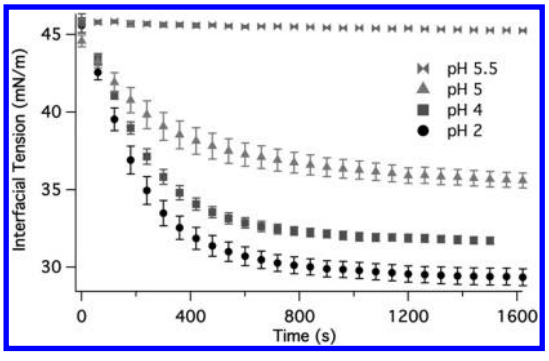

Figure 4. Interfacial tension data for 3 kD sPMA (5 ppm) at different pH values as a function of time.

dx.doi.org/10.1021/la4021096 | *Langmuir* 2013, 29, 10980–10989

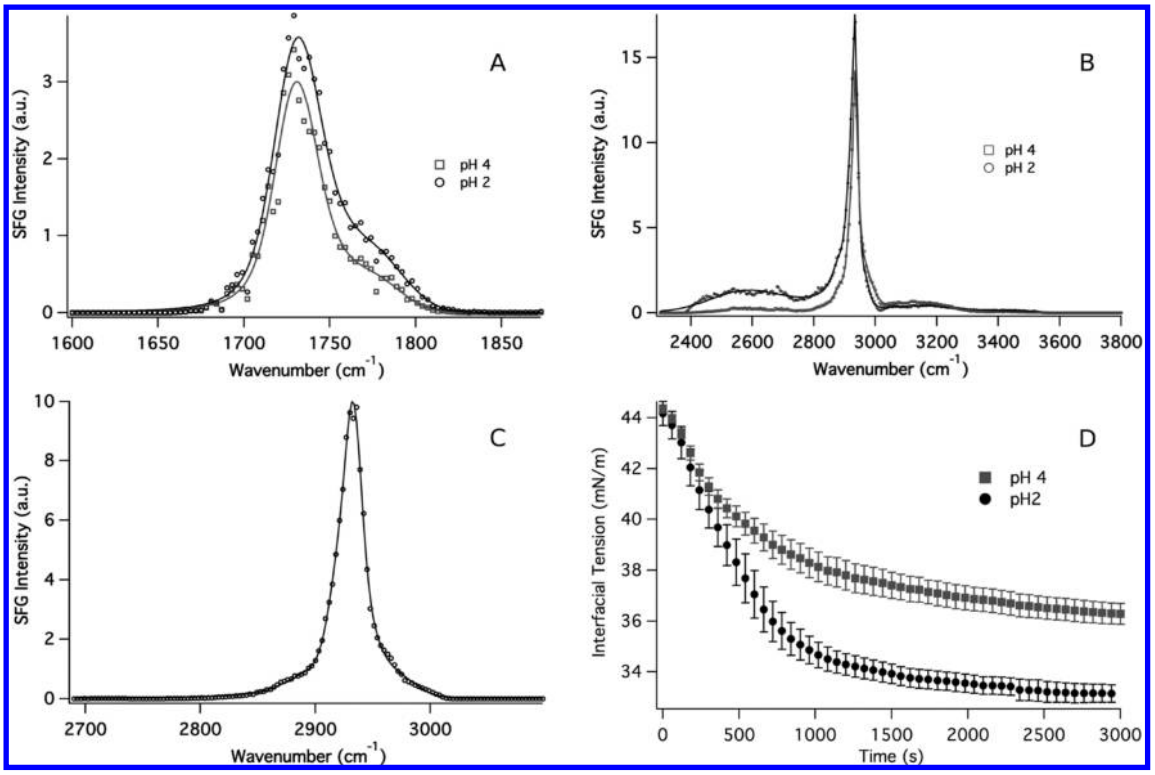

Figure 5. VSF spectra (ssp polarization) and interfacial tension data for 28 kD sPMA (5 ppm) at pH 4, 2, and pD 2. (A) VSF spectra of the carbonyl stretching region. (B) VSF spectra of the CH and OH stretching region. (C) VSF spectra of 28 kD sPMA in D_2O of the CH stretching region. (D) Interfacial tension data as a function of time. Solid lines are fits to the data.

signal is not indicative of disordered sPMA at the interface. We attribute this lack of polymer adsorption at higher pH values to the charge on the polymer making water solvation more favorable than adsorption. The equilibrium interfacial tension values decrease slightly as the pH is decreased from 5 to 2. The equilibrium interfacial tension value is ~35 mN/m at pH 5, ~32 mN/m at pH 4, and ~29 mN/m at pH 2. This indicates that the relative amount of 3 kD sPMA adsorbed to the CCl_4–H_2O interface slightly increases from pH 5 to 2.

Interestingly, the interfacial tension measurements take ~10 min to reach equilibrium for all pH values. In contrast, the VSF signal intensity does not show a similar slow rise but instead reaches a constant value within 1 min of interface preparation as seen in Figures 2 and 3. This behavior has been observed in our previous studies of PAA[34−36] and indicates that the VSF experiment detects only the oriented polymer layer that immediately adsorbs to the interface. What adsorbs over time is disordered material that cannot be detected with VSF spectroscopy but can be detected with interfacial tension measurements. We attribute this behavior to the inherent electric field present at the CCl_4–H_2O interface that is known to assist in the adsorption of ions.[40] This field assists in the quick adsorption of highly oriented material to the oil–water interface. This field, however, does not penetrate deeply enough into the bulk water to orient the more slowly adsorbing material, which then adsorbs in a disordered fashion. These disordered polymers, however, continue to adsorb to the interface because of favorable hydrophobic interactions between the topmost ordered layer and disordered material that subsequently adsorbs.

What is apparent is that a decrease in pH leads to both an increase in the total amount of polymer adsorbed to the interface, as seen in the interfacial tension data, and an increase in the number of ordered carboxylic acid groups that comprise the initially adsorbed polymer layer, as seen in the VSF data. In the first case, the increase in the total amount of polymer adsorbed at the interface is attributed to more favorable hydrophobic interactions between the initially adsorbed polymer layer and the more slowly adsorbing disordered polymer layer. This is due to fewer charges on the polymer chains as the carboxylate groups become protonated, leading to fewer charge–charge repulsion interactions between the initially adsorbed layer and the more slowly adsorbing layer. Likewise, the decrease in pH and subsequent protonation of carboxylate groups lead to an increase in the number of carboxylic acid groups on the polymer chains. Along with the greater ability for the initially adsorbed polymer to pack tightly at the interface as a result of minimized charge–charge repulsions, the larger number of carboxylic acid groups is most likely what contributes to the increase in VSF signal as the pH of the solution is decreased.

Overall, the VSF spectroscopic and interfacial tension data lead to a picture in which a pH change from 5 to 2 results in a slight increase in the total amount of adsorbed 3 kD sPMA at the interface, specifically, the amount of disordered polymer that adsorbs to the interface after the initial adsorption of an ordered polymer layer. This pH decrease additionally leads to a decrease in the amount of charge at the interface and subsequently an increase in the degree of oriented carboxylic acid groups on the polymer chains that initially adsorb to the interface. The water-solvated carboxylate groups are unable to line up at the interface because they adopt opposite orientations on the polymer chains to minimize charge–charge repulsions. Once these groups are protonated and their charges

dx.doi.org/10.1021/la4021096 | Langmuir 2013, 29, 10980–10989

are neutralized, the resulting carboxylic acid groups are able to orient themselves normal to the interface, with the carbonyl groups pointing into both the oil phase and the water phase and with the OH groups pointing into the water phase.

High-Molecular-Weight sPMA. VSF spectra and interfacial tension data were also taken for 28 kD sPMA at varying pH values to elucidate the effect of charge distribution among polymer chains on interfacial adsorption and assembly. Described below and shown in Figure 5 are the VSF spectra for the samples at pH 2 and 4 (A, B) as well as at pD 2 (C). Data were also obtained at pH 3, and the results fall within the trend of the other solutions studied. These data were not included in the figure for the sake of clarity.

Figure 5A shows the VSF spectra of the carbonyl stretching region. At pH 4 and 2, the spectra appear similar to the 3 kD sPMA data. Again, two peaks are present and are attributed to carbonyl groups in a more water-rich environment (1730 cm^{-1}) and carbonyl groups in a more oil-rich environment (1790 cm^{-1}). As the pH decreases from 4 to 2, the amplitudes of both peaks increase, consistent with an increase in the number of oriented carbonyl groups at the interface that was also seen in the 3 kD sPMA VSF spectroscopic data of the carbonyl stretching region.

Small differences can be seen, however, in the CH stretching region of the 28 kD sample compared to that of the 3 kD sample. A spectrum of the 28 kD sample was taken in D_2O at pD 2 (Figure 5C), and the fitting parameters were compared to the corresponding spectrum for the 3 kD sample (Figure 3B) in order to elucidate the cause of the differences between the two spectra. The spectra were fit using a global routine in which all parameters were held constant except for peak amplitudes and Gaussian widths. Peak frequencies were constrained to be within the error from fits of each individual spectrum. Results from the fits indicate that the only significant difference between the two spectra is a decrease in the peak amplitude near 2880 cm^{-1} (assigned to the CH_3 symmetric stretching mode) for the 28 kD sample. We attribute this to the smaller number of polymer end groups at the interface for the 28 kD sample compared to the number for the 3 kD sPMA sample rather than a change in the overall orientation of interfacial methyl groups. This is supported by the fact that the amplitude of the peak near 2980 cm^{-1} (assigned to the CH_3 antisymmetric stretching mode) is the same within the error between the 28 and 3 kD sPMA data. Because both the 28 and 3 kD sPMA samples were prepared at the same monomer concentration, the 28 kD sPMA samples contain about 10 times fewer chains in solution than the 3 kD sPMA samples. The data are therefore consistent with the fact that the 28 kD sPMA sample has 10 times fewer polymer end groups than the 3 kD sPMA sample.

The corresponding H_2O spectra for both polymer sizes show very similar behavior from pH 4 to 2. For the 28 kD sPMA sample, the H_2O spectra in Figure 5B were fit using the same method as described for the 3 kD sPMA H_2O spectra shown in Figure 3A. Results from the fits show an increase in oriented carboxylic acid groups from pH 4 to 2, with an amplitude increase of the peak assigned to the carboxylic acid OH stretching mode (2540 cm^{-1}). Additionally, there is a slight decrease in the amplitude of the peak assigned to the water OH stretching mode near 3200 cm^{-1}, again indicating a decrease in interfacial water structure due to charge neutralization of the interfacial polymer as the pH decreases from 4 to 2. There is, however, an insignificant change in the amplitude of the peak near 3400 cm^{-1} as the pH decreases from 4 to 2. This is not surprising because the change in amplitude of this peak in the H_2O spectra of the 3 kD sPMA sample was not very large. Finally, small-amplitude changes in the CH stretching mode peaks as the pH decreases indicate a change in backbone orientation as the carboxylic acid groups become more ordered at the interface.

Interfacial tension data were also collected for the 28 kD sPMA sample and are shown in Figure 5D. Again, the equilibrium interfacial tension of the pH 2 sample (~33 mN/m) is slightly lower than that of the pH 4 sample (~36 mN/m), suggesting that there is an increase in the amount of disordered polymer adsorbed to the interface as the pH is decreased. Although it is obvious that the interfacial tension of the 28 kD sPMA sample takes nearly 1 h longer to reach equilibrium than the 3 kD sPMA, this is not surprising. It has been observed in studies of different molecular weight polymers that polymer accumulation at fluid interfaces is limited by diffusion, with the time required for interfacial tension values to reach equilibrium longer for larger polymers than for smaller polymers.[35,55]

Overall, at pH ≤4 the 28 and 3 kD sPMA polymers behave very similarly at the CCl_4–H_2O interface, with the strong VSF signal due to the high degree of order of the polymer methylene backbone, carboxylic acid, and methyl groups at the interface. For both sPMA sizes, a decrease in pH results in an increased degree of order of the carboxylic acid groups, with the carbonyl groups able to reside in both oil-rich and water-rich environments. Although the dynamics of the interfacial tension is different between the two sizes, both polymers show a time dependence that is not seen in the VSF spectroscopic data that indicates the fast adsorption of highly oriented polymer chains to the interface followed by the accumulation of disordered material at the interface.

The adsorption behavior for the two differently sized polymers was observed to be different in the pH region from 4 to 5. The adsorption of the 28 kD sPMA to the CCl_4–H_2O interface occurs only at pH <5, as indicated by the similarity of both the OH stretching region spectrum and the interfacial tension value (~44 mN/m) to those of the neat CCl_4–H_2O interface. However, the 3 kD sPMA does adsorb to the interface at pH 5, showing a strong VSF signal and a significant reduction in interfacial tension compared to that of the neat CCl_4–H_2O interface.[53,54]

Between pH 4 and 5, the 28 kD sPMA does adsorb to the interface, yet the polymer interfacial behavior in this pH region is very different than it is for pH ≤4. This is apparent from the time dependence of the VSF signal seen for samples studied in the pH 4 to 5 region. A plot of the VSF signal at 2940 and 1730 cm^{-1} as a function of time is shown in Figure 6 for a 28 kD sPMA sample at pH 4.4.

As can be seen, the intensity of the signal at both 1730 cm^{-1} (carbonyl stretching mode region) and 2940 cm^{-1} (CH stretching mode region) initially increases with time. Once maximum intensity is reached, the signal intensity suddenly decreases until a constant value is reached. This behavior is similar for samples studied between pH 4.2 and 4.9. In contrast, at pH 2–4, signal is observed within ~2 min of interfacial preparation once data collection begins and remains at the same value for ~3 h when data collection is complete. Because a change in VSF signal intensity can be due to either a change in the numbers of molecules at the interface or a change in the orientation of interfacial molecules or both of these factors, interfacial tension data are essential for elucidating the cause of

dx.doi.org/10.1021/la4021096 | Langmuir 2013, 29, 10980–10989

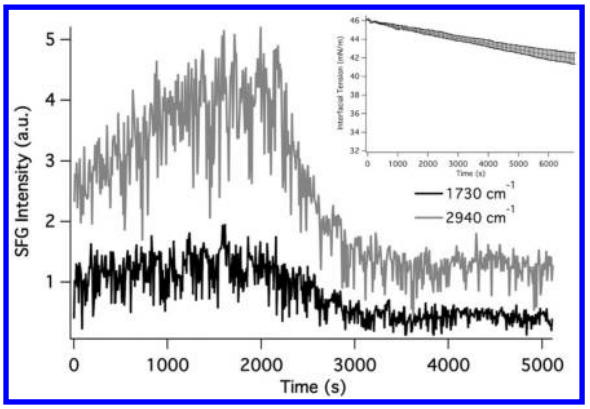

Figure 6. VSF signal intensity (ssp polarization) at 1730 cm^{-1} corresponding to the carbonyl stretching mode region and 2940 cm^{-1} corresponding to the CH stretching mode region as a function of time for 28 kD sPMA (5 ppm) at pH 4.4. The inset is the interfacial tension data as a function of time for the corresponding solution.

signal intensity changes. The interfacial tension data for the 28 kD sPMA at pH 4.4 are shown in the inset of Figure 6. As can be seen, the interfacial tension value continues to decrease with time even after the VSF signal intensity reaches its constant value at a much earlier time. This indicates that the adsorption of polymer to the interface continues over the time period in which changes are seen in the VSF signal intensity. Although this suggests that the initial increase in VSF signal intensity is due to an increase in the number of oriented polymer segments through adsorption to the interface, the decrease in signal is due to polymer reorientation rather than desorption. We attribute the decrease in interfacial tension after the VSF signal intensity reaches equilibrium to the accumulation of disordered polymer to the interface, albeit less than what was observed for the lower-pH samples in which the interfacial tension value for the pH 4.4 sample is ~42 mN/m at 6000 s whereas the value for the pH 2 sample is ~33 mN/m at 3000 s.

The VSF spectra of the carbonyl stretching region and the CH/OH stretching region, shown in Figure 7A,B, indicate that the topmost layer of 28 kD sPMA absorbed to the interface between pH 4 and 5 is quite different than at pH ≤4.

As with the VSFS data taken in the carbonyl stretching region at pH ≤4, the spectrum in Figure 7A was fit to a peak near 1730 cm^{-1} (carbonyl groups in a water-rich environment) and near 1790 cm^{-1} (carbonyl groups in an oil-rich environment). The result of the fit shows that the intensities of the 1730 and 1790 cm^{-1} peaks for the sample at pH 4.4 are much less than what was seen for the lower-pH samples. This is represented in the inset of Figure 7A and indicates that overall there are fewer oriented carbonyl groups at the interface for the pH 4.4 sample compared to the number for the lower-pH samples. The spectrum of the CH/OH stretching region (Figure 7B) confirms this picture. It is quite obvious that the peak near 2540 cm^{-1} attributed to the carboxylic acid OH stretching mode is absent in this spectrum whereas a strong signal due to the coordinated water OH stretching mode is present. Additionally, the peak near 3668 cm^{-1} is assigned to the free OH stretching mode and indicates that there is not complete coverage of the interface by the polymer,[56] consistent with the relatively high interfacial tension values. This mode was not present for samples of 28 kD sPMA at pH ≤4, indicative of full coverage of the interface. Finally, the intensities of the CH stretching mode peaks are much weaker

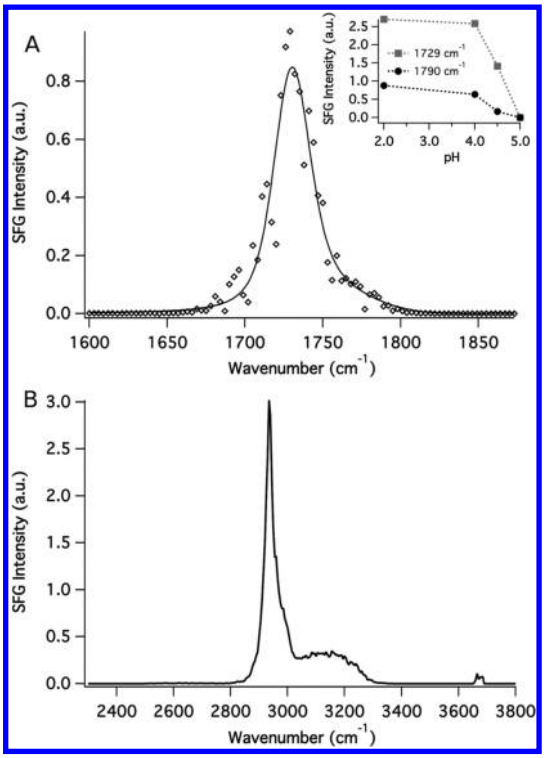

Figure 7. Equilibrium VSF spectra (ssp polarization) of 28 kD sPMA (5 ppm) at pH 4.4 in the carbonyl stretching region (A) and CH and OH stretching region (B). The inset shows the fit amplitudes for the peaks at 1730 and 1790 cm^{-1} as a function of pH.

for the pH 4.4 sample compared to those for the lower-pH samples, consistent with the carbonyl stretching mode data.

A picture consistent with the data discussed above for the 28 kD sPMA samples between pH 4 and 5 is one in which ordered polymer chains initially adsorb to the interface, with continued adsorption of oriented material until a critical point. At this point, chain segments rearrange at the interface until an equilibrium polymer surface structure is attained that is more disordered than the initially adsorbed polymer. After this point, disordered polymer continues to adsorb to the interface, yet this accumulation does not lead to complete coverage of the interface. For 3 kD sPMA between pH 4 and 5, full coverage of the interface occurs within minutes of interface preparation, as observed by both the strong VSF signal attributed to the polymer along with the lack of a peak at ~3668 cm^{-1} attributed to the free OH stretching mode. A constant VSF signal at both ~1730 and ~2940 cm^{-1} indicates no rearrangement of the initially adsorbed polymer layer with time. Again, the decrease in the interfacial tension value with time indicates the accumulation of disordered polymer at the interface with time.

It is obvious that between pH 4 and 5 the polymer chain length plays a role in sPMA interfacial adsorption behavior. As stated in the Introduction, the charge distribution among polymer chains for the 28 kD sPMA samples, with ~326 monomers per chain, will be different than the charging of the 3 kD sPMA samples, with ~34 monomers per chain. The solutions were made with the same number of monomers such that at 5 ppm, solutions of both 28 kD sPMA and 3 kD sPMA have a monomer concentration of ~0.06 mM. This results in the 3 kD solutions containing overall ~10 time the number of polymer chains in solution as the 28 kD solutions. Because of this, the 3 kD samples contain a relatively large number of

dx.doi.org/10.1021/la4021096 | Langmuir 2013, 29, 10980−10989

chains in solution in which a small number of charges can accumulate on each chain, whereas the 28 kD samples contain a relatively small number of chains in solution in which a large number of charges accumulate on each chain.

To give an idea of the approximate number of charges per chain as the solution pH decreases from 5 to 2, titration data for sPMA from previous work by Kawaguchi et al. will be discussed.[57] At pH ∼5, approximately 20% of monomers in solution will be charged, corresponding to ∼7 charges/chain for the 3 kD sPMA (34 monomers/chain) and ∼65 charges/chain for the 28 kD sPMA (326 monomers/chain). At pH ∼4, approximately 5% of monomers in solution will be charged, corresponding to ∼1 charge/chain for the 3 kD sPMA and ∼16 charges/chain for the 28 kD sPMA. By pH 3, only approximately 1% of monomers in solution will be charged, corresponding to less than 1 charge/chain for the 3 kD sPMA and ∼3 charges/chain for the 28 kD sample. That the larger sPMA can accumulate so many more charges per chain than the smaller sPMA between pH 4 and 5 appears to play a key role in the greater surface activity of the 3 kD sPMA compared to that of the 28 kD sPMA in this pH range.

Previous work on polyelectrolytes in bulk aqueous solution has suggested that cooperative effects allow charges on polymer chains to accumulate near each other.[58] In our previous study, this effect was used to explain why PAA desorbed so readily from the CCl_4–H_2O interface in a very narrow pH region and specifically that deprotonation occurred on carboxylic acid functional groups near each other such that sections of the chain became so hydrophilic that solvation was more favorable than adsorption.[34−36] We conclude that the same effect is at play here with the two differently sized sPMA polymers. As discussed above, the 28 kD sPMA is able to accumulate more charges per chain than the 3 kD sPMA polymer. These charges have the ability to accumulate near each other on the chain, creating sections of the polymer that are very hydrophilic. The result is that when both polymer solutions are at the same pH the larger polymer will be more hydrophilic than the smaller polymer. This explains why the smaller polymer is able to adsorb to the CCl_4–H_2O interface at higher pH values than the larger polymer.

Additionally, this polyelectrolyte charging behavior explains the time dependence of the VSF signal observed for the 28 kD sPMA between pH 4 and 5. For the sPMA samples where there is no observed time dependence of the VSF signal, the polymer chains are able to adsorb and spread out at the interface so quickly that these steps are not observed in the spectroscopy. The disordered polymer that continues to adsorb to the interface is observed only in the interfacial tension data. For the 28 kD sPMA between pH 4 and 5, however, the hydrophilic nature of the polymer causes the adsorption of oriented material to be quite slow. Despite the hydrophilic nature of 28 kD sPMA at this pH, the initial adsorption of oriented polymer segments is assisted by the inherent electric field present at the CCl_4–H_2O interface.[40] Once a critical amount of polymer adsorbs to the interface (i.e., when the VSF signal is at a maximum), the reorientation of polymer occurs until an equilibrium surface structure is reached. Because of the accumulation of charges near each other on the polymer chain, it is likely that the critical amount of polymer adsorption correlates to a critical amount of highly charged chain sections at the interface. The reorientation of these sections would thus be due to the solvation of these highly charged chain sections to minimize the charge−charge repulsions that would be present if these chains were spread out in an extended configuration at the oil−water interface.

Because the interfacial tension does not change much for these systems compared to that for the lower-pH samples, it shows that the degree of polymer accumulation after the topmost equilibrium surface layer is attained is much less than for the lower-pH 28 kD sPMA samples. This is consistent with the fact that the multilayer adsorption is ascribed to favorable hydrophobic interactions between the topmost adsorbed layer and the disordered material that subsequently adsorbs to the interface.[34−36] This has also been noted in adsorption studies of biological polyelectrolytes.[59,60] For the 28 kD sPMA in the pH region from 4 to 5, these favorable hydrophobic interactions are minimal as a result of the highly hydrophilic nature of the polymer.

A cartoon depicting the surface structure of the 3 kD and 28 kD sPMA polymers between pH 4 and 5 is shown in Figure 8.

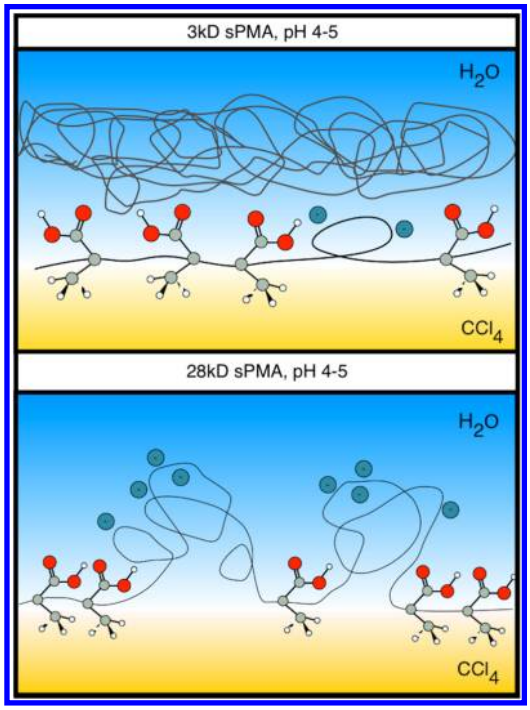

Figure 8. Cartoon depicting the interfacial behavior of sPMA at 5 > pH > 4 for the 3 kD polymer (top) and the 28 kD polymer (bottom).

Overall, the smaller 3 kD sPMA polymer adsorbs to the interface at lower pH values than does the 28 kD sPMA polymer. Specifically, for the 3 kD sPMA polymer, a change in pH from 5 to 2 results in only a gradual increase in the ordering of carboxylic acid groups as the carboxylate groups become protonated as well as an increase in the amount of disordered polymer adsorbed to the interface. The 28 kD sample, however, experiences different pH-dependent adsorption behavior. In the region from pH 4 to 5, adsorption is followed by polymer chain reorientation to minimize charge−charge interactions and is due to the ability of the 28 kD sPMA polymer to accumulate more charges on the chains compared to the 3 kD sPMA polymer. In the region of pH ≤4 for 28 kD sPMA, the polymer adsorption behavior is very similar to that of the 3 kD sPMA polymer. By this point, charge accumulation on the chain must be minimal so that polymer adsorption and accumulation at the interface are more favorable than both complete solvation and

dx.doi.org/10.1021/la4021096 | *Langmuir* 2013, 29, 10980−10989

polymer chain reorientation in solvating highly charged chain sections.

CONCLUSIONS

Through VSF spectroscopic and interfacial tension measurements, we observe for the first time how the distribution of charges among differently sized polymer chains in solution influences polyelectrolyte behavior at an oil−water interface. The differences between the interfacial behavior of the large and small sPMA polymers only occur in a narrow pH range, from pH 4 to 5. For the larger sPMA polymer in this pH range, the ability to accumulate a greater number of charges per chain compared to the smaller sPMA polymer makes the larger polymer overall more hydrophilic; the highly charged chain segments of the larger adsorbed polymer protrude into the aqueous phase and do not allow full coverage of the interface. In contrast, the smaller polymer, with only a few charges per chain, is better able to pack at the interface. Overall, the smaller polymer appears to behave more like an alkyl surfactant than does the larger polymer.

The sensitivity of these polyelectrolyte systems to specific solution conditions has implications for oil recovery and environmental remediation processes that utilize the adsorption of natural polyelectrolytes to an oil−water interface. By fine-tuning factors such as macromolecular size and the placement of ionizable groups, it seems possible to engineer natural polyelectrolyte mimetics and analogs that will accumulate at the oil−water interface under any set of environmental conditions. Because natural polyelectrolyte substances are known to be polydisperse and structurally very complex, it may also be possible to select specific sizes and structures of humic or fulvic acids that will behave ideally at environmental oil−water interfaces, either for the purpose of recovering a natural fuel source or for remediating water contaminated by toxic materials. Our future work on the isotactic PMA isomer will further demonstrate the sensitivity of interfacial adsorption and assembly on both polyelectrolyte and bulk solution characteristics.

AUTHOR INFORMATION

Corresponding Author

*E-mail: richmond@uoregon.edu. Fax: 541-346-3422. Phone: 541-346-0116.

Notes

The authors declare no competing financial interest.

ACKNOWLEDGMENTS

The work has been supported by the U.S. Department of Energy, Office of Basic Energy Sciences, Division of Materials Sciences and Engineering under award DE-FG02-96ER45557. We thank Fred Moore for his editorial contributions.

REFERENCES

(1) Voet, D.; Voet, J. G.; Pratt, C. W. *Fundamentals of Biochemistry: Life at the Molecular Level*; Wiley: New York, 2006.

(2) Zhang, J.; Li, G.; Yang, F.; Xu, N.; Fan, H.; Yuan, T.; Chen, L. Hydrophobically Modified Sodium Humate Surfactant: Ultra-Low Interfacial Tension at the Oil/Water Interface. *Appl. Surf. Sci.* **2012**, *259*, 774−779.

(3) van Stempvoort, D. R.; Lesage, S. Binding of Methylated Naphthalenes to Concentrated Aqueous Humic Acid. *Adv. Environ. Res.* **2002**, *6*, 495−504.

(4) van Stempvoort, D. R.; Lesage, S.; Novakowski, K. S.; Millar, K.; Brown, S.; Lawrence, J. R. Humic Acid Enhanced Remediation of an Emplaced Diesel Source in Groundwater. 1. Laboratory-Based Pilot Scale Test. *J. Contam. Hydrol.* **2002**, *54*, 249−276.

(5) Rebhun, M.; Meir, S.; Laor, Y. Using Dissolved Humic Acid to Remove Hydrophobic Contaminants from Water by Complexation-Flocculation Process. *Environ. Sci. Technol.* **1998**, *32*, 981−986.

(6) Quadri, G.; Chen, X.; Jawitz, J. W.; Tambone, F.; Genevini, P.; Faoro, F.; Adani, F. Biobased Surfactant-Like Molecules from Organic Wastes: The Effect of Waste Composition and Composting Process on Surfactant Properties and on the Ability to Solubilize Tetrachloroethene (PCE). *Environ. Sci. Technol.* **2008**, *42*, 2618−2623.

(7) Wang, Y.; Zhang, Y.; Du, W.; Wu, C.; Zhao, J. Intelligent Core-Shell Nanoparticles and Hollow Spheres Based on Gelatin and PAA Via Template Polymerization. *J. Colloid Interface Sci.* **2009**, *334*, 153−160.

(8) Kwon, H. J.; Gong, J. P. Negatively Charged Polyelectrolyte Gels as Bio-Tissue Model System and for Biomedical Application. *Curr. Opin. Colloid Interface Sci.* **2006**, *11*, 345−350.

(9) Chanda, A.; Fokin, V. V. Organic Synthesis "On Water". *Chem. Rev.* **2009**, *109*, 725−748.

(10) Jung, Y.; Marcus, R. A., Protruding Interfacial OH Groups and 'On-Water' Heterogeneous Catalysis. *J. Phys.: Condens. Matter* **2010**, *22*.

(11) Ovejero, J. M.; Fernandez, R. A.; Dassie, S. A. Ion Transfer across Liquid/Liquid Interface under Forced Hydrodynamic Conditions. I: Digital Simulations. *J. Electroanal. Chem.* **2012**, *666*, 42−51.

(12) Kihara, S.; Kasuno, M.; Okugaki, T.; Shirai, O.; Maeda, K. Biomimetic Charge Transfer Reactions at the Aqueous/Organic Solution Interface or through Artificial Membrane. *Electrochemistry* **2012**, *80*, 390−400.

(13) Hu, L. F.; Chen, M.; Fang, X. S.; Wu, L. M. Oil-Water Interfacial Self-Assembly: A Novel Strategy for Nanofilm and Nanodevice Fabrication. *Chem. Soc. Rev.* **2012**, *41*, 1350−1362.

(14) Niu, Z.; He, J.; Russell, T. P.; Wang, Q. Synthesis of Nano/Microstructures at Fluid Interfaces. *Angew. Chem., Int. Ed.* **2010**, *49*, 10052−10066.

(15) Boker, A.; He, J.; Emrick, T.; Russell, T. P. Self-Assembly of Nanoparticles at Interfaces. *Soft Matter* **2007**, *3*, 1231−1248.

(16) Huang, J. S.; Varadaraj, R. Colloid and Interface Science in the Oil Industry. *Curr. Opin. Colloid Interface Sci.* **1996**, *1*, 535−539.

(17) Fayer, M. D. Dynamics of Water Interacting with Interfaces, Molecules, and Ions. *Acc. Chem. Res.* **2012**, *45*, 3−14.

(18) Boucher, J.; Trudel, E.; Methot, M.; Desmeules, P.; Salesse, C. Organization, Structure and Activity of Proteins in Monolayers. *Colloids Surf., B* **2007**, *58*, 73−90.

(19) Ash, P. A.; Bain, C. D.; Matsubara, H. Wetting in Oil/Water/Surfactant Systems. *Curr. Opin. Colloid Interface Sci.* **2012**, *17*, 196−204.

(20) Watarai, H.; Teramae, N.; Sawada, T. *Interfacial Nanochemistry: Molecular Science and Engineering at Liquid-Liquid Interfaces*; Kluwer Academic/Plenum Publishers: New York, 2005.

(21) Beaman, D. K.; Robertson, E. J.; Richmond, G. L. From Head to Tail: Structure, Solvation, and Hydrogen Bonding of Carboxylate Surfactants at the Organic-Water Interface. *J. Phys. Chem. C* **2011**, *115*, 12508−12516.

(22) Jerman, B.; Kogej, K. Fluorimetric and Potentiometric Study of the Conformational Transition of Isotactic and Atactic Poly-(methacrylic acid) in Mixed Solvents. *Acta Chim. Slov.* **2006**, *53*, 264−273.

(23) Jerman, B.; Podlipnik, C.; Kogej, K. Molecular Dynamics Simulation of Poly(methacrylic acid) Chains in Water. *Acta Chim. Slov.* **2007**, *54*, 509−516.

(24) Jerman, B.; Breznik, M.; Kogej, K.; Paoletti, S. Osmotic and Volume Properties of Stereoregular Poly(methacrylic acids) in Aqueous Solution: Role of Intermolecular Association. *J. Phys. Chem. B* **2007**, *111*, 8435−8443.

(25) Dong, J.; Ozaki, Y.; Nakashima, K. Infrared, Raman, and Near-Infrared Spectroscopic Evidence for the Coexistence of Various

Hydrogen-Bond Forms in Poly(acrylic acid). *Macromolecules* **1997**, *30*, 1111−1117.
(26) Tajiri, T.; Morita, S.; Ozaki, Y. Hydration Mechanism on a Poly(methacrylic acid) Film Studied by In Situ Attenuated Total Reflection Infrared Spectroscopy. *Polymer* **2009**, *50*, 5765−5770.
(27) Dong, J.; Tsubahara, N.; Fujimoto, Y.; Ozaki, Y.; Nakashima, K. Fourier Transform Infrared Studies of pH- and Temperature-Dependent Conformational Changes of Solid Poly(methacrylic acid). *Appl. Spectrosc.* **2001**, *55*, 1603−1609.
(28) Vermohlen, K.; Lewandowski, H.; Narres, H. D.; Koglin, E. Adsorption of Polyacrylic Acid on Aluminium Oxide: Drift Spectroscopy and Ab Initio Calculations. *Colloids Surf., A* **2000**, *170*, 181−189.
(29) Vermohlen, K.; Lewandowski, H.; Narres, H. D.; Schwuger, M. J. Adsorption of Polyelectrolytes onto Oxides - The Influence of Ionic Strength, Molar Mass, and Ca^{2+} Ions. *Colloids Surf., A* **2000**, *163*, 45−53.
(30) Chen, Y. X.; Liu, S. Y.; Wang, G. Y. Kinetics and Adsorption Behavior of Carboxymethyl Starch on Alpha-Alumina in Aqueous Medium. *J. Colloid Interface Sci.* **2006**, *303*, 380−387.
(31) Bykov, A. G.; Lin, S.-Y.; Loglio, G.; Miller, R.; Noskov, B. A. Kinetics of Adsorption Layer Formation in Solutions of Polyacid/Surfactant Complexes. *J. Phys. Chem. C* **2009**, *113*, 5664−5671.
(32) Stamkulov, N. S.; Mussabekov, K. B.; Aidarova, S. B.; Luckham, P. F. Stabilisation of Emulsions by Using a Combination of an Oil Soluble Ionic Surfactant and Water Soluble Polyelectrolytes. I: Emulsion Stabilisation and Interfacial Tension Measurements. *Colloids Surf., A* **2009**, *335*, 103−106.
(33) Paul, H. J.; Corn, R. M. Second-Harmonic Generation Measurements of Electrostatic Biopolymer-Surfactant Coadsorption at the Water/1,2-Dichloroethane Interface. *J. Phys. Chem. B* **1997**, *101*, 4494−4497.
(34) Beaman, D. K.; Robertson, E. J.; Richmond, G. L. Metal Ions: Driving the Orderly Assembly of Polyelectrolytes at a Hydrophobic Surface. *Langmuir* **2012**, *28*, 14245−14253.
(35) Beaman, D. K.; Robertson, E. J.; Richmond, G. L. Ordered Polyelectrolyte Assembly at the Oil-Water Interface. *Proc. Natl. Acad. Sci. U.S.A.* **2012**, *109*, 3226−3231.
(36) Beaman, D. K.; Robertson, E. J.; Richmond, G. L. Unique Assembly of Charged Polymers at the Oil-Water Interface. *Langmuir* **2011**, *27*, 2104−2106.
(37) Wang, Z.; Fu, L.; Yan, E. C. Y. C−H Stretch for Probing Kinetics of Self-Assembly into Macromolecular Chiral Structures at Interfaces by Chiral Sum Frequency Generation Spectroscopy. *Langmuir* **2013**, *29*, 4077−4083.
(38) Eisenberg, H. Thermodynamics and the Structure of Biological Macromolecules - Rozhinkes-Mit-Mandeln. *Eur. J. Biochem.* **1990**, *187*, 7−22.
(39) Roger, G. M.; Durand-Vidal, S.; Bernard, O.; Meriguet, G.; Altmann, S.; Turq, P. Characterization of Humic Substances and Polyacrylic Acid: A High Precision Conductimetry Study. *Colloids Surf., A* **2010**, *356*, 51−57.
(40) McFearin, C. L.; Richmond, G. L. The Role of Interfacial Molecular Structure in the Adsorption of Ions at the Liquid-Liquid Interface. *J. Phys. Chem. C* **2009**, *113*, 21162−21168.
(41) Bain, C. D.; Davies, P. B.; Ong, T. H.; Ward, R. N.; Brown, M. A. The Structure of Interfaces Probed by Sum-Frequency Spectroscopy. *Surf. Interface Anal.* **1991**, *17*, 529−530.
(42) Lim, M.; Hochstrasser, R. M. Unusual Vibrational Dynamics of the Acetic Acid Dimer. *J. Chem. Phys.* **2001**, *115*, 7629−7643.
(43) Goates, S. R.; Schofield, D. A.; Bain, C. D. A Study of Nonionic Surfactants at the Air−Water Interface by Sum-Frequency Spectroscopy and Ellipsometry. *Langmuir* **1999**, *15*, 1400−1409.
(44) Brown, M. G.; Raymond, E. A.; Allen, H. C.; Scatena, L. F.; Richmond, G. L. The Analysis of Interference Effects in the Sum Frequency Spectra of Water Interfaces. *J. Phys. Chem. A* **2000**, *104*, 10220−10226.
(45) Ota, S. T.; Richmond, G. L. Uptake of SO_2 to Aqueous Formaldehyde Surfaces. *J. Am. Chem. Soc.* **2012**, *134*, 9967−9977.
(46) Lin-Vien, D. *The Handbook of Infrared and Raman Characteristic Frequencies of Organic Molecules*; Academic Press: Boston, 1991.
(47) Raczynska, E. D.; Duczmal, K.; Darowska, M. Experimental (FT-IR) and Theoretical (DFT-IR) Studies of Keto-Enol Tautomerism in Pyruvic Acid. *Vib. Spectrosc.* **2005**, *39*, 37−45.
(48) Conboy, J. C.; Messmer, M. C.; Richmond, G. L. Investigation of Surfactant Conformation and Order at the Liquid-Liquid Interface by Total Internal Reflection Sum-Frequency Vibrational Spectroscopy. *J. Phys. Chem.* **1996**, *100*, 7617−7622.
(49) Guyot-Sionnest, P.; Hunt, J. H.; Shen, Y. R. Sum-Frequency Vibrational Spectroscopy of a Langmuir Film: Study of Molecular Orientation of a Two-Dimensional System. *Phys. Rev. Lett.* **1987**, *59*, 1597−1600.
(50) Mitsui, K.; Ukaji, T. *Infrared Spectra of Some Aqueous Solutions*; Research Reports of Ikutoku Tch. Univ., 1977, B-2.
(51) Gragson, D. E.; Richmond, G. L. Probing the Intermolecular Hydrogen Bonding of Water Molecules at the CCl_4/Water Interface in the Presence of Charged Soluble Surfactant. *J. Chem. Phys.* **1997**, *107*, 9687−9690.
(52) Ong, S. W.; Zhao, X. L.; Eisenthal, K. B. Polarization of Water-Molecules at a Charged Interface - 2nd Harmonic Studies of the Silica Water Interface. *Chem. Phys. Lett.* **1992**, *191*, 327−335.
(53) Freitas, A. A.; Quina, F. H.; Carroll, F. A. Estimation of Water-Organic Interfacial Tensions. A Linear Free Energy Relationship Analysis of Interfacial Adhesion. *J. Phys. Chem. B* **1997**, *101*, 7488−7493.
(54) Apostoluk, W.; Drzymala, J. An Improved Estimation of Water-Organic Liquid Interfacial Tension Based on Linear Solvation Energy Relationship Approach. *J. Colloid Interface Sci.* **2003**, *262*, 483−488.
(55) Zhang, J.; Pelton, R. The Dynamic Behavior of Poly(N-Isopropylacrylamide) at the Air/Water Interface. *Colloids Surf., A* **1999**, *156*, 111−122.
(56) Scatena, L. F.; Richmond, G. L. Isolated Molecular Ion Solvation at an Oil/Water Interface Investigated by Vibrational Sum-Frequency Spectroscopy. *J. Phys. Chem. B* **2004**, *108*, 12518−12528.
(57) Kawaguchi, S.; Takahashi, T.; Tajima, H.; Hirose, Y.; Ito, K. Preparation, Characterization, and Dissociation Properties of Poly-(acrylic acid) and Poly(methacrylic acid) with Narrow Molecular Weight Distribution. *Polym. J.* **1996**, *28*, 735−741.
(58) Garces, J. L.; Koper, G. J. M.; Borkovec, M. Ionization Equilibria and Conformational Transitions in Polyprotic Molecules and Polyelectrolytes. *J. Phys. Chem. B* **2006**, *110*, 10937−10950.
(59) Beverung, C. J.; Radke, C. J.; Blanch, H. W. Adsorption Dynamics of L-Glutamic Acid Copolymers at a Heptane/Water Interface. *Biophys. Chem.* **1998**, *70*, 121−132.
(60) Beverung, C. J.; Radke, C. J.; Blanch, H. W. Protein Adsorption at the Oil/Water Interface: Characterization of Adsorption Kinetics by Dynamic Interfacial Tension Measurements. *Biophys. Chem.* **1999**, *81*, 59−80.